JVST B
Journal of Vacuum Science & Technology B

Outgassing rate testbed for in-operation analysis of powered and heated assemblies

Cite as: J. Vac. Sci. Technol. B **40**, 044203 (2022); https://doi.org/10.1116/6.0001898
Submitted: 01 April 2022 • Accepted: 16 June 2022 • Published Online: 13 July 2022

Marvin Warner, Michael Elsen, Lisa Wörner, et al.

JVST B
Journal of Vacuum Science & Technology B

ARTICLE

avs.scitation.org/journal/jvb

Outgassing rate testbed for in-operation analysis of powered and heated assemblies

Cite as: J. Vac. Sci. Technol. B **40**, 044203 (2022); doi: 10.1116/6.0001898
Submitted: 1 April 2022 · Accepted: 16 June 2022 ·
Published Online: 13 July 2022

Marvin Warner,[1,a)] Michael Elsen,[1] Lisa Wörner,[2] Claus Braxmaier,[2,3] and Jens Grosse[1]

AFFILIATIONS

[1]Center of Applied Space Technology and Microgravity (ZARM), University of Bremen, 28359 Bremen, Germany
[2]Institute for Quantum Technologies, German Aerospace Center (DLR), Söflinger Straße 100, 89077 Ulm, Germany
[3]Institute of Microelectronics, Ulm University, 88091 Ulm, Germany

[a)]**Author to whom correspondence should be addressed:** marvin.warner@zarm.uni-bremen.de

ABSTRACT

We introduce a new apparatus for measuring the outgassing rate of assemblies and functional units. Outgassing rates given in the literature, if available, are mostly insufficient to plan and set up a vacuum system, more so if commercial parts, preassembled items, or complex electronics with unknown components are deployed. Outgassing rates have a severe impact on the required pumping speed in ultrahigh vacuum systems and they change if the samples are powered or heated. The newly built apparatus uses the throughput method to measure outgassing rates. It can house probes with a size of $0.10 \times 0.10 \times 0.13\,\mathrm{m}^3$ and supplies electrical currents of up to 5 A. In addition, a heater can establish temperatures of up to 200 °C directly. A procedure is given to identify the main gas inputs and to retrieve data with a lower limit of $1.5 \times 10^{-8}\,\mathrm{Pa\,m^3\,s^{-1}}$ after 100 h in vacuum. In this paper, we present the experimental setup and first results for samples of polytetrafluorethylene, polyamide (PA6), Viton (1A), and oxygen-free high thermal conductivity copper at room temperature.

I. INTRODUCTION

Ultrahigh vacuum (UHV) is important for fundamental physics and engineering applications, for example, systems that use quantum phenomena for precision measurements, such as BECCAL,[1] MAIUS,[2] CAL,[3] or MAQRO.[4] Those systems require pressures below 1×10^{-8} Pa to operate. The achievable pressure is limited by the gas inputs and the used pump system. In typical metal-sealed UHV systems, the outgassing rate is the dominating gas load. Since miniaturized pump systems cannot supply high pumping rates, the knowledge of the outgassing behavior under different temperatures becomes crucial to achieve low pressures.

Outgassing rates of various materials have already been investigated.[5–8] However, the literature values for outgassing rates of any given material are prone to differ from one source to another, sometimes as severely as spanning orders of magnitude. These discrepancies are caused by various factors, such as the surface roughness, prevailing time under vacuum, or pretreatment.[9]

Quantum technologies, such as cold atom experiments, often use electrical components inside the vacuum system. An atom chip, for instance, can generate magnetic fields in close proximity to cooled atoms,[2] while a piezodriven stage allows for tip and tilt optics inside the vacuum.[1] Here, various materials are joined by different processes in order to connect the components, which can lead to severely different outgassing rates, occurrence of cavities, or other factors contributing to deviations from the planned achievable vacuum pressure. The applied electrical currents result in an increase in the temperature, finally resulting in an increase in the outgassing rate. Thus, it provokes an elevated pressure near the field of interest (e.g., cooled atoms) and reduces the performance of the experiments.[10]

We developed an outgassing rate testbed that can measure probes as well as assemblies with arbitrary geometries and has the ability to simulate different applicable operational scenarios. This paper shall give an extensive look into the apparatus and will be used as the baseline for upcoming measurements.

We will give a short introduction to the outgassing phenomena in Sec. I A and an insight into the limitations of current literature values in Sec. I B. In Sec. II, a short explanation of the experimental method is given, which results in a detailed description of the design in Sec. III. Section IV presents the measurement results and discussion for first empty chamber and material sample tests for verification of the test setup.

A. Outgassing rates

Once a material is exposed to vacuum, the surface bounded gas starts to desorb from the surface. In fact, gas molecules are released with a certain outgassing rate (Q), which represents the overlap of diffusion, desorption, permeation, adsorption, and absorption kinetics.[11] Typically, the outgassing rate is normalized to the geometrical surface area (A), which yields the surface specific outgassing rate (q).

The amount of gas molecules in the material change with time, which in turn changes the outgassing rates. Hence, q is expressed as a time dependent property q_t. A well known empirical power law decay of q_t is caused by the depletion of the gas source, and it can be measured for most of the outgassing materials of interest in this work.[5,12] Equation (1) is well known and, for instance, presented by Dylla *et al.*[12] The equation describes the development of the outgassing rate over time

$$q_t = q_0 \cdot (t + t_0)^{-n}. \tag{1}$$

An outgassing rate q_t at time t and the exponential decay index n are introduced. The parameters q_0, t_0, and n can be found from fitting experimental data to Eq. (1).

B. Literature values

A multitude of factors, such as the surface roughness, the pretreatment, and many more, cause a vast spectrum in the literature values of the outgassing rate per material. Thus, the calculation of outgassing rate prior to installation becomes difficult. To illustrate this, outgassing rates for chosen materials are plotted in a violin plot in Fig. 1.

Figure 1 grants a quantitative probability distribution of the outgassing rate. Additional information is given by the heat map, which shows the time under vacuum for the probes. Not all sources state a time under vacuum, therefore a not applicable (n.a.) coloring was implemented. Furthermore, mechanical and heat treatments are not considered in the plot, as they are not quantifiable and often not given. Recent literature surveys pointed to the influence of material thickness, which are as well neglected here.[6,13]

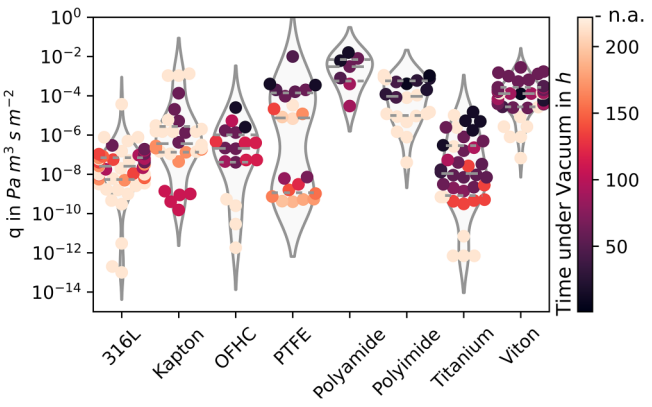

FIG. 1. Literature survey of outgassing rates for different materials. Colorbar shows the time under vacuum stated in the corresponding literature. Sources are given in Table I. n.a. (not applicable)—identifies values that have no information about the time under vacuum. Note: Some values are fitted from given equations in the literature (color online).

Table I summarizes the literature values visualized in Fig. 1. It demonstrates the difficulty of choosing values for a vacuum system design in progress that reflects the material and treatment of the implemented parts. For metals such as stainless steel (316L), Battes *et al.*[5] studied different processes and derived a range of 2.96×10^{-7}–4.16×10^{-8} Pa m^3 s^{-1} m^{-2} for the outgassing rate at 10 h in vacuum. Saitoh *et al.*,[15] on the other hand, found an outgassing rate of 3.7×10^{-5} Pa m^3 s^{-1} m^{-2} for a simply cleaned 316L probe before baking at 10 h, while Akimichi and Hirata[14] showed that with a TiN coating, the outgassing rate can be suppressed to 1×10^{-13} Pa m^3 s^{-1} m^{-2}. Polymers such as Viton, polyimide, polyamide, and polytetrafluorethylene (PTFE) are more difficult to predict as they depend on too many parameters. For instance, the difference between the maximum and minimum for PTFE is seven orders of magnitude (see Table I).

All those findings are not in disagreement as there is either a pretreatment, a different methodology, a coating, or another inherent difference involved. Moreover, it has to be mentioned that plenty of literature values are available for common UHV chamber materials, such as stainless steel, allowing one to isolate the outgassing rate for a well defined and treated material with good precision. However, not all parameters can be reflected in Fig. 1, so it reflects a distorted picture of the literature data.

In many systems, these materials are joined in assemblies, where common heat and surface treatments are inapplicable, due to requirements of optical coatings or sensitive electronics. As described before, this strongly impacts the expected outgassing rate, which is further complicated by the absence of information on outgassing behavior of joined or powered parts. This, in turn, renders the calculation or estimation of the final outgassing rate infeasible and unreliable. It is impossible to investigate all parameters (pretreatment, surface finish, etc.) for all technical materials, and the alternative is to measure the outgassing rates of the assemblies prior to installation. We present a setup to measure the outgassing rate in full operation conditions.

TABLE I. Minima and maxima of outgassing rates from literature. Literature values as presented in Fig. 1. Note: Some values are fitted from given equations in the literature.

	q in Pa m^3 s^{-1} m^{-2}		
Material	Minimum	Maximum	Reference
316L	1.00×10^{-13}	3.70×10^{-05}	5, 14–19
Kapton	1.52×10^{-10}	1.33×10^{-03}	6, 20, 21
OFHC	1.81×10^{-12}	2.51×10^{-05}	7, 19, 21–24
PTFE	4.00×10^{-10}	1.00×10^{-02}	7, 21, 25–29
Polyimide	4.00×10^{-08}	1.10×10^{-03}	6, 21, 30
Polyamide	3.00×10^{-05}	1.60×10^{-02}	7, 28, 31
Titanium	7.00×10^{-13}	1.51×10^{-05}	7, 9, 19, 29, 32–36
Viton	6.67×10^{-08}	2.80×10^{-03}	5, 28–30, 37

II. METHOD

The outgassing rate of low outgassing samples can be measured via different experimental methods. The throughput and the pressure rise method are the most common for low outgassing samples.[11,38,39] The pressure rise method uses the constant pressure rise of a vacuum vessel after closing the vacuum pump. Thus, the outgassing rate from the chamber walls, or the inherent probe, can be identified at one point in time. Here, the throughput method was implemented since this method allows for the study of the outgassing rate over time. The method uses a constant pumping rate and the splitting of two chambers by an orifice. With a known conductance (C_o) of the orifice, the overall outgassing rate can be derived by Eq. (2). Measurements of the pressure at a chamber that contain the probe (p_{PC}) and the pressure at an analysis section (p_{AS}), which are separated by the orifice, yield the outgassing rate

$$q_t = (p_{PC} - p_{AS}) \cdot \frac{C}{A}. \tag{2}$$

The conductance (C), however, is a function of the vacuum system, orifice geometry, the gas type, and the gas temperature. For an orifice with a circular cross section (A_o) and a length (l_o), a well known analytic approach yields the conductance by Eq. (3),

$$C_o = \frac{\bar{c}}{4} \cdot A_o \cdot P_o. \tag{3}$$

Here, $\bar{c}$ represents the average thermal velocity of the gas molecules and P_o the transmission probability of the orifice.[11] For serial pipe installations, the poor conductance of an orifice is dominant compared to typically used DN40 pipes, which yields $C = C_o$. The effective pumping rate S_{eff} can be derived from Eq. (4). Here, S is the nominal pumping rate at the pump inlet,

$$S_{eff} = \frac{S}{1 + \frac{S}{C_o}}. \tag{4}$$

The throughput method is limited by the transient, nontrivial background outgassing of the chamber. This includes, among others, the effects of venting processes, temperature changes, and (re)-adsorption of gas molecules from the probes. Other limitations on the throughput method are the used instruments, such as the vacuum pumps, the orifice, or the vacuum gauges. Gas-specific signals of ionization gauges, for instance, have to be considered. Grinham and Chew[9] point out the advantages and disadvantages. The throughput method offers the opportunity to measure time dependent outgassing phenomena, which is decisive for in-operation measurements.

III. OUTGASSING MEASUREMENT TESTBED

A. Test setup

The test setup consists of vacuum chambers, a measurement and control unit, and a transfer mechanism for the probe-holder. The three elements will be described in the following sections. A simplified flow chart is given in Fig. 2.

1. Vacuum chamber

The apparatus is divided into three main sections: the gate chamber (GC), the probe chamber (PC), and the analysis section (AS), as shown in Fig. 2. The main sealing technique is based on bakable Con-Flat (CF) flanges according to ISO standard 3669.

The gate chamber and the probe chamber are two identical systems made from stainless steel (316L). Both were surface finished by an electropolishing process. One chamber can

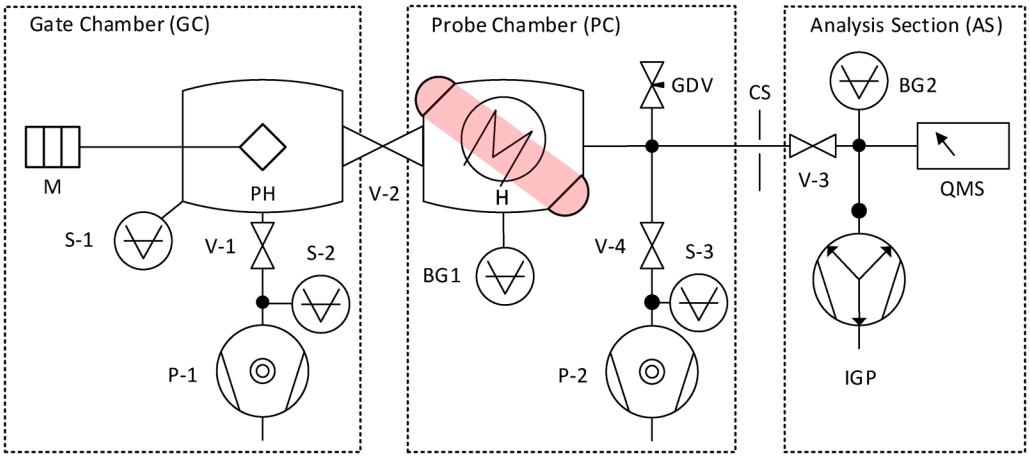

FIG. 2. Flow chart of the outgassing measurement testbed: BG—Barion hot cathode gauge, CS—conductance slit (Orifice), GC—gate chamber, GDV—gas dosing valve, H—heater, IGP—ion getter pump, P—turbomolecular pump, PH—probe-holder, QMS—quadropule mass spectrometer, S—pressure sensor, V—gate valve. Red shaded area represents optical access on opposite sides (color online).

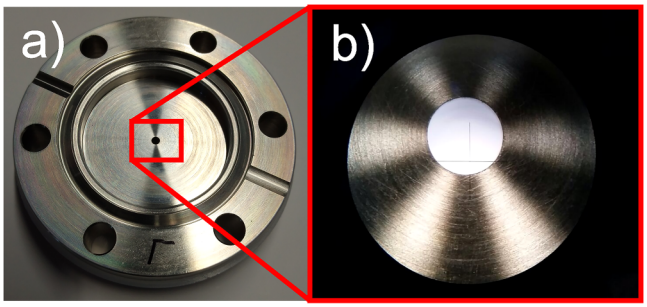

FIG. 3. Orifice characteristics. (a) Photo of the CF DN40 aperture after machining. (b) View through the *Quadra-Chek QC200* on the orifice.

accommodate samples of up to 0.250 m in height and a diameter of 0.155 m.

CF DN40 connections are used to attach two $67 \times 10^{-3}\ m^3\ s^{-1}$ turbomolecular pumping stations (P-1 and P-2). The connection to the test chamber is established by a gate valve (V-3). An orifice (CS) is installed in front of V-3. A magnetic coupled manipulator (M), electrical feedthroughs, two optical accesses, a gas dosing valve (GDV), and the vacuum gauges (BG1 and S-3) are implemented.

CF DN160 ports connect the gate chamber and the probe chamber with a gate valve (V-2). A quick access door at the gate chamber and a viewport at the probe chamber enable the implementation of the probe. The suspension (probe-holder) limits the probe size to $0.10 \times 0.10 \times 0.13\ m^3$.

The analysis section consists of stainless steel piping. It allows for the connection of a quadrupol mass spectrometer (QMS), one vacuum gauge (BG2), and a $40 \times 10^{-3}\ m^3\ s^{-1}$ ion getter pump (IGP, by *Agilent Technologies*), with a saturation pumping rate of $25 \times 10^{-3}\ m^3\ s^{-1}$ for N_2.

The orifice is a machined CF DN40 aperture. Figure 3(a) shows the aperture. The machined hole diameter was measured with a *Quadra-Chek QC200 (by Metronics)* yielding a diameter of $d_o = 2205 \times 10^{-3} \pm 7 \times 10^{-6}$ m. The view through the ocular of the Quadra-Check is shown in Fig. 3(b). The conductance is calculated by the hole cross section with Eq. (3). With the given diameter, the orifice conductance $[C_O(N_2)]$ was calculated to $3.11 \times 10^{-4}\ m^3\ s^{-1}$ for N_2 and a gas temperature of 293.15 K. The gas temperature and type influences the conduction and, thus, affects the measurements. Considering only the effect of the gas type an outgassing of only H_2 results in an underestimation of the conduction by a factor of 3.7 compared to N_2.

2. Measurement and control unit

The analysis section houses the measurement unit for the data acquisition. It is constantly pumped down via the $40 \times 10^{-3}\ m^3\ s^{-1}$ ion getter pump. Additionally, a vacuum gauge [BG2, hot cathode ionization, by *VACOM* (Ref. 40)] to measure the pressure (p_{AS}) is connected. An identical gauge connects to the probe chamber (BG1). The measurement range is 1×10^{-9}–1×10^{5} Pa with an accuracy of 10% for lower pressure ranges (<1 Pa). All values are measured as N_2 equivalent.

A QMS (*QMG 220 Prisma Plus*[41]) allows for the analysis of the gas composition up to 200 amu. The QMS is used in a scan mode for a first estimation of the gas composition. A multi-ion detection (MID) scan, for the most abundant mass to charge ratios, can be applied additionally. This procedure allows for a timed resolution of the outgassing composition.

The control unit for monitoring, data logging, heating, electrical power, and the control of the overall test setup is placed inside a 19 in. rack.

3. Probe-holder and transfer mechanism

The gate chamber features a quick access door, which allows for probe installation. While the gate chamber is vented with dry N_2 to install the probe, the probe and the test chamber are sealed by the gate valve (V-2). Thus, contamination of the main vacuum chambers is decreased and repeatability of measurements is enhanced.

The suspension of the probe (probe-holder) is attached to a magnetic coupled manipulator arm (M). This arm is able to horizontally transfer into the probe chamber. Here, a probe-mount is installed, which offers the mechanical and electrical interface to the probe-holder. Included is a ceramic heater (H), a Type-K control temperature sensor, and connections to the electrical feedthroughs. The manipulator arm enables the mechanical and electrical connection by a rotating coupling mechanism.

The probe-holder is equipped with five powerlines, offering up to 5 A per pin, and two Type-K thermocouples. The electric connection is enabled by a ceramic D-Sub connector. All connections for power, monitoring, and heating are connected to UHV-feedthroughs via kapton isolated cables.

Figure 4 shows the setup of an exemplary probe inside the gate chamber. The circular disk was fixed to the probe-holder

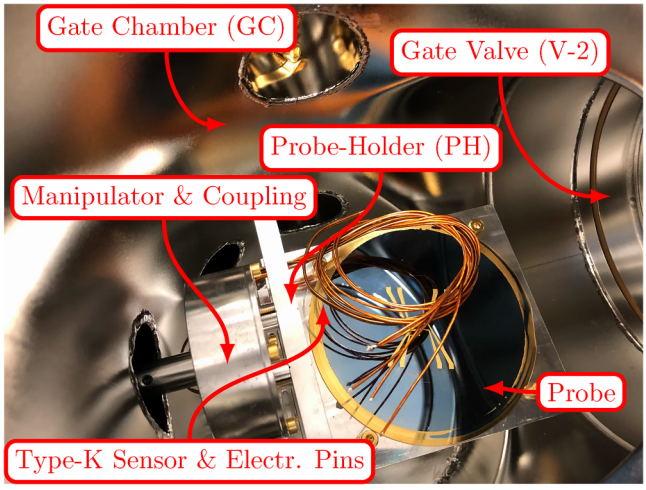

FIG. 4. Exemplary probe installed with vacuum suitable screws on the probe-holder. The probe-holder is connected to the coupling mechanism. Type-K temperature sensors and electrical pins are not connected and freely floating.

using UHV suitable screws. In this case, the Type-K sensors and electrical pins were not connected.

B. Test procedure

The steps of a repeatable measurement procedure for the outgassing testbed are shown in Fig. 5.

Step 1:
The background outgassing of the probe chamber, without a sample, is determined in background measurement no. 1 (BM1). BM1 usually runs from 1 to 24 h. An analog scan with the QMS is performed to find the most abundant residual gases in the vacuum system.

Step 2:
BM1 is stopped by opening the gate valve (V-4) to the turbomolecular pump (P-2) and subsequently closing the valve to the test chamber (V-3). After a short wait time, the valve (V-2) is opened and the probe-holder is transferred to the gate chamber. V-2 is closed and the gate chamber is vented with dry N_2.

Step 3:
The probe is cleaned according to the desired processes and mounted on the probe-holder. The Type-K temperature sensors are placed and fixed. Finally, the electric connections are established by screw terminals. This process usually takes 15–30 min, depending on the complexity of the setup. During the implementation of the probe, a second background measurement (BM2) is performed without the influence of the probe-holder.

Step 4:
Finally, the gate chamber is evacuated via the pump (P-1). Typically, a pressure of 1×10^{-1} Pa is reached in below 1 min. The evacuation of the gate chamber is monitored and after the pressure reached 1×10^{-2} Pa, BM2 is stopped. The test chamber is closed (V-3) and the gate is opened (V-2) to transfer the probe-holder. After successful coupling and retraction of the manipulator, arm V-2 is closed. An additional check of the pressure inside the probe chamber is implemented before opening V-3 to not contaminate the analysis section. The process from first evacuation of the gate chamber to the start of the probe measurement usually takes 2–6 h.

Step 5:
Subsequently, the test chamber is opened (V-3) and the valve to the turbomolecular pump is closed (V-4) in order to begin the actual measurement (AM). A QMS analog scan is performed after 1 h. The mass spectrum is analyzed up to 200 amu. Most abundant mass ratios are chosen to be measured in a MID scan. The probe is measured for a predefined measurement time. A temperature profile (T) and an electrical current (I) are applied during the AM.

Steps 6–9:
In order to investigate the influence of the probe-holder, a final background measurement is performed. Therefore, the probe-holder is transferred back to the gate chamber analog to the previously described transfer. An in-between measurement is started (BM3), while the probe is removed from the probe-holder. The empty holder is transferred to the probe chamber and BM4 is started. This measurement is used as a baseline for the outgassing rate. The same mounting elements, electrical currents, and temperature profiles are applied to the system. All used insulated cables are connected in an electrical short in vacuum. To resemble the AM, the probe itself is connected in-line with the vacuum cables but operated outside the vacuum system.

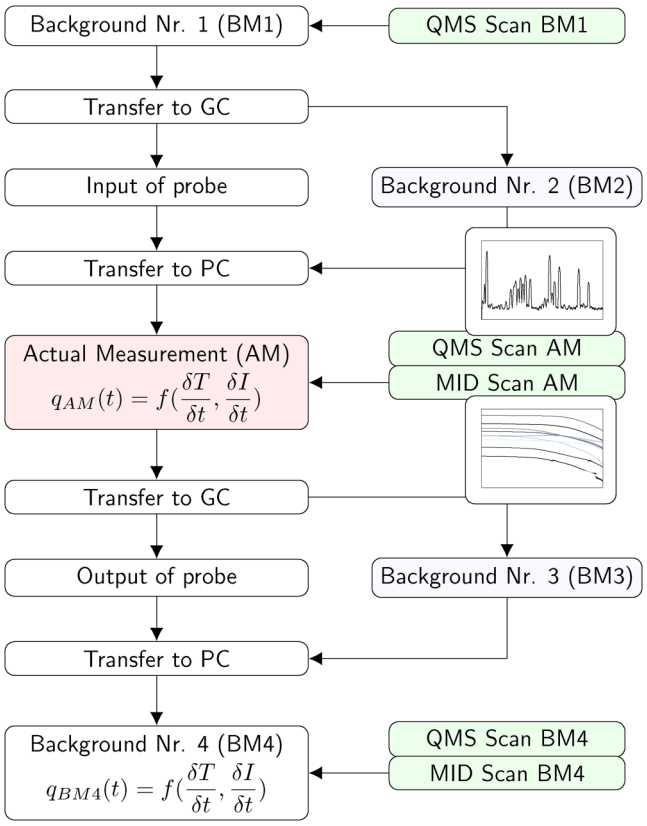

FIG. 5. Simplified flow chart of the measurement procedure. GC—gate chamber, PC—probe chamber, QMS—quadrupole mass spectrometer, MID—multi-ion detection.

All vacuum parts are baked out before the first measurements at 120 °C for a duration of a minimum of one week. In between two measurements, all chambers are pumped for >100 h. Additionally, another week of bake-out is performed if the background pressure has changed.

C. Uncertainties

The uncertainty of the two hot cathode ionization gauges (BG1) and (BG2) is 10% for the low pressure regime, while the calculation for the surface areas of the probes inherits an uncertainty of ∼2%. The diameter used to calculate the conductance by Eq. (3) has an uncertainty of $\sim 7 \times 10^{-6}$ m. The error propagation according to the standard for evaluation of measurement data[42] yields an uncertainty of ∼12% with a coverage factor of $k = 2$. The uncertainty is calculated for each measurement point independently and plotted as a shaded area.

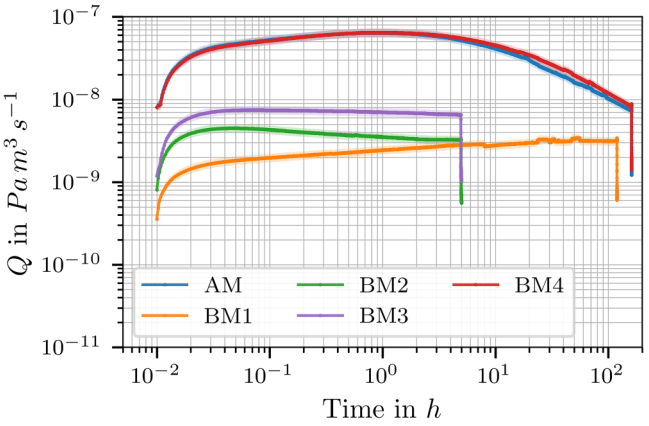

FIG. 6. Empty chamber test with the process of Fig. 5 followed as if a probe would have been inserted (venting process of gate chamber between AM and BM4). Time for venting the gate chamber was 30 min. BM—background measurement, AM—actual measurement.

Additionally, the aforementioned impact of gases readsorbing on the chamber walls is present. Thus, BM4 and BM1 become of interest. Due to the adsorbed molecules, at the components in vacuum, the measured outgassing rate is higher than in reality. In Sec. IV A, it is shown that BM4 yields a conservative approach to evaluating the impact given by the chamber. So, it becomes useful to show the corrected outgassing rate q_c,

$$q_c = q_{AM} - q_{BM4}. \tag{5}$$

In Sec. IV C, one can see that there is a high impact for low outgassing samples such as PTFE.

IV. MEASUREMENTS AND RESULTS

The outgassing rate of material samples was measured. The results are presented in Sec. IV C. However, prior to the sample measurements, an empty chamber measurement was performed to evaluate the background outgassing rate. The results are presented in Sec. IV A.

A. Empty chamber measurements

The background outgassing desorbing from the probe-chamber, -holder, and -mount is not negligible. Empty chamber measurements were performed to identify the behavior of the chamber and define the process parameters. Therefore several tests were performed for a full sample measurement. This includes venting of the gate chamber with N_2 for 30 min, unhinging the probe-holder, and vice versa.

In Fig. 6, a typical empty chamber measurement is plotted. The x axis shows the time, beginning with insertion into the probe chamber, in a logarithmic scale. A shaded area depicts the uncertainties, which are described in Sec. III C. The data were cropped at the closing time of the gate valve V-4. Three important pieces of information can be found from Fig. 6:

(1) The background outgassing of the system is time dependent and varies from 1.5×10^{-8} to 7×10^{-8} Pa m^3 s^{-1}.
(2) Venting the gate chamber has a contaminating effect on the background. In the first 100 h, the background is $>1 \times 10^{-8}$ Pa m^3 s^{-1}.
(3) The AM and BM4 show the same trend, with respect to the given uncertainties. BM4 of the empty chamber is slightly higher for measurement times >30 h.

Following that observation, the background of the chamber shall be modeled as a time depending function in line with Eq. (1). In a least squares fit, the decay index n was found to be 0.857, the offset outgassing q_{off} is 5.78×10^{-7} Pa m^3 s^{-1} h^{-1}, and the offset time t_{off} yields 12.12 h.

Figure 6 shows a high agreement of BM4 and AM, despite the additional venting process of the gate chamber and the probe-holder. This effect was seen in all empty chamber measurements that were performed. We investigated this effect and found that the cause is the contamination of the probe-holder due to the venting and installation process. However, with the given measures of Fig. 5, we can quantify this influence. Nevertheless, the background outgassing is limiting our system to probes with an outgassing rate equal or higher than 7×10^{-8} Pa m^3 s^{-1} at 10 h and 1.5×10^{-8} Pa m^3 s^{-1} at 100 h.

B. Material samples

A set of material samples with given literature values were chosen. The probe samples have different flat geometries: Viton (1A), polyamide (PA6), oxygen-free high thermal conductivity (OFHC) copper are circular disks, while PTFE is a rectangular plate. The samples, the geometry, the vacuum-exposed surface areas, the expected outgassing rate (q_{expect}), and the manufacturer are given in Table II. The order year and the treatment give a first impression on the history of the probe. Until the measurement all probes were

TABLE II. Tested material samples. q_{expect} indicates the expected outgassing rate taking the minimum and maximum literature outgassing values from Table I, combined with the given surface area A_{double}. Order year is 2020 for all samples. All samples were wiped with IPA before testing.

Probe ID	A_{single} (10^{-4} m^2)	A_{double} (10^{-4} m^2)	Thickness (10^{-3} m)	q_{expect} (Pa m^3 s^{-1} m^{-2})	Supplier
Polytetrafluorethylene (PTFE)	108	208	2	1.92×10^{-08}–4.80×10^{-1}	Goodfellow
Viton (1A)	84.82	163.36	2	4.08×10^{-6}–1.71×10^{-1}	Hokosil
Polyamide (PA6)	84.82	163.36	2	2.45×10^{-6}–6.73×10^{-2}	Hokosil
OFHC copper (99.99%)	85.14	163.86	2.1	1.10×10^{-10}–1.53×10^{-3}	MaTeck

stored in a controlled laboratory environment: air temperature 22 °C and 25% relative humidity. The flat probes were mounted directly on to the probe-holder; thus, two surface areas are given: the single sided surface (A_{single}), which has a surface-vacuum area which is obscured by the probe-holder, and the overall geometric area (A_{double}) of the material sample. For all values, A_{double} is used as reference.

C. Outgassing results

The probes from Table II were tested sequentially. All probes were cleaned with a clean room wipe and isopropanol (IPA). Furthermore, the surface was visually checked and subsequently blown with dry air. The probes were inserted in the gate chamber and fixed to the probe-holder. Cleaned, vented, and gold plated screws, which were kept in the vacuum system for the whole measurement cycle of Fig. 5, were used. The outgassing data are plotted in Fig. 7, while the respective surface area can be found in Table II.

An empty chamber measurement is plotted in addition and is divided by the depicted surface area in order to show the limitations of the apparatus. Finally, the plot shows the uncertainty (see Sec. III C) of the measurement in a shaded area. The measured and the corrected outgassing rates are both shown; the latter are visible only for the PTFE and OFHC samples. These dotted lines show the corrected outgassing rate q_c as described in Sec. III C. Table III summarizes the outgassing rates at 25, 50, and 100 h.

As expected, the polymers (Viton, PA 6 and PTFE) have a high initial outgassing rate compared to the OFHC sample. OFHC is, with the used probe geometry, below the limit of the measurement capability. Thus, only a maximum outgassing rate for the sample is given considering the background outgassing. PTFE has the highest reduction of the outgassing rate over time. In the first 50 h, the outgassing was higher than $\sim 1 \times 10^{-5}$ Pa m^3 s^{-1} m^2, while after 100 h, the outgassing rate dropped to the detection limit of the outgassing testbed. The highest outgassing rate was measured for PA 6. All probes are well in line with the expected outgassing rate, presented in Table II.

In addition to the outgassing rate, we measured the qualitative contribution of gases with a QMS. Figure 8 shows the blank measurement of the background (BM1) and the AM for PA6. Shown

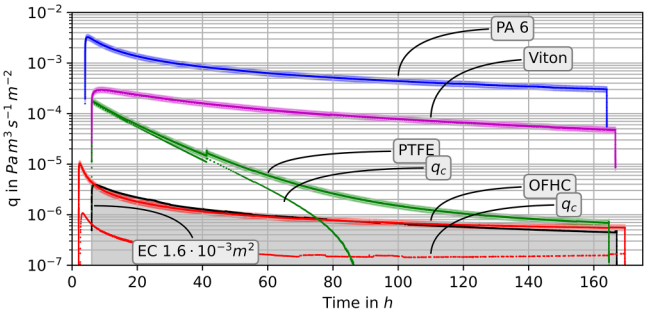

FIG. 7. Outgassing rate measurement of different untreated samples at 293.15 K. Shaded areas show the measurement uncertainty. The uncertainty was evaluated at all point of read-outs. The thin dotted lines show the corrected outgassing rate q_c. EC—empty chamber.

TABLE III. Outgassing rate measurement of different untreated samples at room temperature. Derived from Fig. 7.

	q in Pa m^3 s^{-1} m^{-2}		
Probe	q_{25}	q_{50}	q_{100}
PTFE	4.21×10^{-5}	9.99×10^{-6}	$<1.50 \times 10^{-6}$
Viton (1A)	2.13×10^{-4}	1.37×10^{-4}	7.84×10^{-5}
PA6	1.16×10^{-3}	7.28×10^{-4}	4.40×10^{-4}
OFHC	$<1.56 \times 10^{-6}$	$<1.01 \times 10^{-6}$	$<6.90 \times 10^{-7}$

are the intensity profiles, which is the ion current of any mass to charge ratio (m z^{-1}) in percent of the highest ion current found for m z^{-1}.

For BM1, the most abundant gas is H_2 (m z^{-1} = 2). However, the amount of N_2/CO (m z^{-1} = 28) is roughly 50% of the H_2 ion current. For AM, a high amount of water (H_2O) is detected, which leads back to the bounded water in the probe.

D. Discussion

From the presented data and the first test runs, information of the setup can be derived. The contamination of the chamber walls and the probe-holder have a non-negligible impact on measurements, especially if the probe surfaces are small and the outgassing rate is low. However, with the procedure discussed in Sec. III B the influence can be quantified. Furthermore, the QMS scan yields information about the origin of gases and, thus, increasing the confidence in the results.

The testbed is capable of measuring probes starting from 2 h under vacuum. From first tests, we identified that the implemented heater works as expected. This allows for heating the probes independently of the overall chamber. Finally, the contacting of probe-mount and probe-holder is functioning, and, thus, assemblies could operate inside our chamber during any measurement.

Certainly, the focus of the presented system is not the measurement of ultralow outgassing material samples, but the

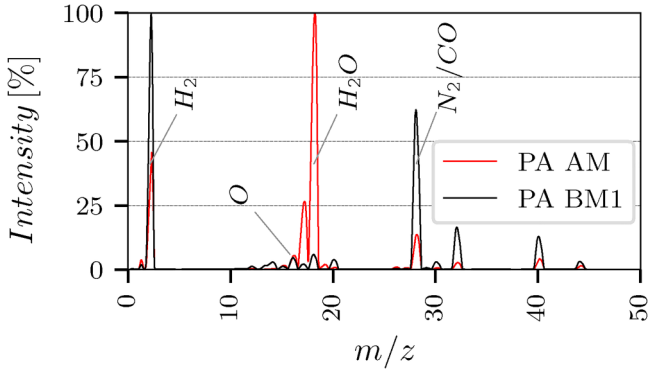

FIG. 8. QMS scan of the PA 6 probe after 5 h of pumping. Intensity profile for the ion currents of BM1 and AM.

accumulated outgassing of assemblies operating in vacuum can be investigated. This enables the observation of overlapping effects like temperature, electrical current, and joining technologies that could not be calculated from existing literature values.

V. CONCLUSION

In this paper, an outgassing testbed that uses the throughput method to measure outgassing rates is presented. Samples with a total outgassing rate higher than 1.5×10^{-8} Pa m^3 s^{-1} after 100 h and a pressure dependent uncertainty of ~12% can be detected. Probe geometries can fit in a cube with maximum side length of $0.10 \times 0.10 \times 0.13$ m^3 Additionally, the apparatus allows for inserting complex geometries with high surface areas. A geometric surface area of 0.10 m^3 can be achieved easily. Finally, a quadrupole mass spectrometer provides a qualitative study of gas species desorbing from the probes.

The apparatus is tested by measuring well known material probes. Polyamide (PA6), PTFE, OFHC copper, and Viton (1A) were sampled for >150 h each. The measurements are in agreement with the presented range of literature values.

The presented data indicate that, due to numerous influencing factors, outgassing rate literature values for materials are not practical for the design of vacuum systems with integrated assemblies. However, changing pressure distributions and increasing outgassing rates, due to temperature changes or electrical currents, can become debilitating for quantum experiments. Thus, the system offers high flexibility for probe size and geometry. Furthermore, electrical and thermal interfaces allow for powered and heated measurements, allowing for the characterization of assemblies before installation into a vacuum system.

ACKNOWLEDGMENTS

This work was carried out in the framework of the QUANTUS projects. It was supported by the German Space Agency (DLR) with funds provided by the Federal Ministry of Economics and Technology (BMWi) under Grant No. 50WP1701. Additional funds were provided by the Christa and Manfred Fuchs endowed professorship. Support of all team members and the funding entities is highly acknowledged by the authors.

AUTHOR DECLARATIONS

Conflict of Interest

The authors have no conflicts to disclose.

Author Contributions

Marvin Warner: Conceptualization (equal); Data curation (equal); Formal analysis (equal); Investigation (equal); Methodology (equal); Resources (equal); Validation (equal); Visualization (equal); Writing – original draft (equal); Writing – review and editing (equal). **Michael Elsen:** Conceptualization (equal); Data curation (equal); Formal analysis (equal); Investigation (equal); Methodology (equal); Validation (equal); Writing – original draft (equal). **Lisa Wörner:** Conceptualization (equal); Funding acquisition (equal); Methodology (equal); Writing – review and editing (equal). **Claus Braxmaier:** Funding acquisition (equal); Supervision (equal); Writing – review and editing (equal). **Jens Grosse:** Conceptualization (equal); Funding acquisition (equal); Methodology (equal); Project administration (equal); Resources (equal); Supervision (equal); Writing – review and editing (equal).

DATA AVAILABILITY

The data that support the findings of this study are available from the corresponding author upon reasonable request.

REFERENCES

[1]K. Frye *et al.*, EPJ Quantum Technol. **8**, 1 (2021).
[2]D. Becker *et al.*, Nature **562**, 391 (2018).
[3]E. R. Elliott, M. C. Krutzik, J. R. Williams, R. J. Thompson, and D. C. Aveline, npj Microgravity **4**, 16 (2018).
[4]R. Kaltenbaek *et al.*, EPJ Quantum Technol. **3**, 5 (2016).
[5]K. Battes *et al.*, J. Vac. Sci. Technol. A **33**, 021603 (2015).
[6]K. Battes, C. Day, and V. Hauer, J. Vac. Sci. Technol. A **36**, 021602 (2018).
[7]R. J. Elsey, Vacuum **25**, 347 (1975).
[8]V. Hauer, K. Battes, M. Flämmich, V. Ierardi, K. Jousten, and J. Šetina, Vacuum **122**, 250 (2015).
[9]R. Grinham and A. Chew, Appl. Sci. Convergence Technol. **26**, 95 (2017).
[10]P. Shen, K. W. Madison, and J. L. Booth, Metrologia **57**, 025015 (2020).
[11]W. Jitschin, *Handbook of Vacuum Technology* (Wiley-VCH Verlag GmbH & Co. KGaA, Weinheim, 2016), pp. 29–166.
[12]H. F. Dylla, D. M. Manos, and P. H. LaMarche, J. Vac. Sci. Technol. A **11**, 2623 (1993).
[13]S. G. Sammartano, "Outgassing rates of PEEK, Kapton® and Vespel® polymers," M.S. thesis (CERN, Geneva, 2020).
[14]H. Akimichi and M. Hirata, Metrologia **42**, S184 (2005).
[15]M. Saitoh, K. Shimura, T. Iwata, T. Momose, and H. Ishimaru, J. Vac. Sci. Technol. A **11**, 2816 (1993).
[16]R. Nuvolone, J. Vac. Sci. Technol. **14**, 1210 (1977).
[17]M. L. Stutzman *et al.*, AIP Conf. Proc. **671**, 300 (2003).
[18]Y. Ishikawa and T. Yoshimura, J. Vac. Sci. Technol. A **13**, 1847 (1995).
[19]F. Grangeon, C. Monnin, M. Mangeard, and D. Paulin, Vacuum **73**, 243 (2004).
[20]M. Bernardini *et al.*, "Outgassing measurements of kapton insulated cables," VACPISA Virgo Technical Report VACPISA 036 P (1996).
[21]E. A. Moshey, "A compilation of outgassing data on vacuum materials" (Princeton University, Plasma Physics Laboratory, Engineering Technical Memorandum, Princeton, NJ, 1982).
[22]R. M. Yamamoto and J. Harvey, Plasma Phys. Fusion Technol. **11**, 8 (1979).
[23]F. Watanabe, Y. Koyatsu, and H. Miki, J. Vac. Sci. Technol. A **13**, 2587 (1995).
[24]Y. Koyatsu, H. Miki, and F. Watanabe, Vacuum **47**, 709 (1996).
[25]J. Edsparr, "Measurement of PTFE outgassing for the XENON experiment," Technical Report (Harvard University, Cambridge, MA, 2018).
[26]J. P. Gatica, "Outgassing of materials with respect to XENON," (Columbia University Report, New York, 2016).
[27]Y. Luo, X. Wu, K. Wang, and Y. Wang, Mapan-J. Metrol. Soc. I **31**, 61 (2016).
[28]T. J. Patrick, Vacuum **23**, 411 (1973).
[29]T. J. Patrick, Vacuum **31**, 351 (1981).
[30]P. W. Hait, Vacuum **17**, 547 (1967).
[31]A. P. Povilus, C. J. Wurden, Z. Vendeiro, M. Baquero-Ruiz, and J. Fajans, J. Vac. Sci. Technol. A **32**, 033001 (2014).
[32]A. Schram, NASA Tech. Rep. **103**, 55 (1963).
[33]M. Takeda, H. Kurisu, S. Yamamoto, H. Nakagawa, and K. Ishizawa, Appl. Surf. Sci. **258**, 1405 (2011).
[34]Y. Morimoto *et al.*, J. Vac. Soc. Jpn. **45**, 665 (2002).

[35]K. Ishizawa, H. Kurisu, S. Yamamoto, T. Nomura, and N. Murashige, J. Phys. Conf. Ser. **100**, 092023 (2008).
[36]H. Kurisu, G. Kimoto, H. Fujii, and K. Tanaka, J. Vac. Soc. Jpn. **49**, 254 (2006).
[37]L. Chernatony, Vacuum **27**, 605 (1977).
[38]R. J. Elsey, Vacuum **25**, 299 (1975).
[39]P. A. Redhead, J. Vac. Sci. Technol. A **20**, 1667 (2002).
[40]*BARION®-Series Operating Manual* (VACOM Vakuum Komponenten und Messtechnik GmbH, Großlöbichau, 2021).
[41]QMG 220 F1, "PrismaPlus®, 1–100 u, offene Ionenquelle, Y, 200 °C, 0°, IO 220-Modul" (Pfeiffer Vacuum GmbH, Aßlar, 2021).
[42]JCGM-ISO100, "Evaluation of measurement data," in *Guide to the Expression of Uncertainty in Measurement* (Joint Committee for Guides in Metrology, Geneva, 2008).